AD-A119 977   ARMY ELECTRONICS RESEARCH AND DEVELOPMENT COMMAND WS--ETC F/G 4/2
A VERTICAL STRUCTURE ALGORITHM FOR LOW VISIBILITY/LOW STRATUS C--ETC(U)
JUN 82 M G HEAPS.

UNCLASSIFIED ERADCOM/ASL-TR-0111 NL

1 OF 1
AD A
119977

END
DATE
FILMED
11-82
DTIC

(12)

ASL-TR-0111

AD

Reports Control Symbol
OSD - 1366

AD A119977

A VERTICAL STRUCTURE ALGORITHM FOR LOW VISIBILITY/LOW STRATUS CONDITIONS

JUNE 1982

By

Melvin G. Heaps

Approved for public release; distribution unlimited.

US Army Electronics Research and Development Command
Atmospheric Sciences Laboratory
White Sands Missile Range, NM 88002

82 10 07 022

NOTICES

Disclaimers

The findings in this report are not to be construed as an official Department of the Army position, unless so designated by other authorized documents.

The citation of trade names and names of manufacturers in this report is not to be construed as official Government indorsement or approval of commercial products or services referenced herein.

Disposition

Destroy this report when it is no longer needed. Do not return it to the originator.

SECURITY CLASSIFICATION OF THIS PAGE (When Data Entered)

REPORT DOCUMENTATION PAGE

READ INSTRUCTIONS BEFORE COMPLETING FORM

1. REPORT NUMBER ASL-TR-0111	2. GOVT ACCESSION NO. AD-A119977	3. RECIPIENT'S CATALOG NUMBER
4. TITLE (and Subtitle) A VERTICAL STRUCTURE ALGORITHM FOR LOW VISIBILITY/LOW STRATUS CONDITIONS		5. TYPE OF REPORT & PERIOD COVERED Final Report
		6. PERFORMING ORG. REPORT NUMBER
7. AUTHOR(s) Melvin G. Heaps		8. CONTRACT OR GRANT NUMBER(s)
9. PERFORMING ORGANIZATION NAME AND ADDRESS US Army Atmospheric Sciences Laboratory White Sands Missile Range, NM 88002		10. PROGRAM ELEMENT, PROJECT, TASK AREA & WORK UNIT NUMBERS DA Task 1L161102B53A/C
11. CONTROLLING OFFICE NAME AND ADDRESS US Army Electronics Research and Development Command Adelphi, MD 20783		12. REPORT DATE June 1982
		13. NUMBER OF PAGES
14. MONITORING AGENCY NAME & ADDRESS (if different from Controlling Office)		15. SECURITY CLASS. (of this report) UNCLASSIFIED
		15a. DECLASSIFICATION/DOWNGRADING SCHEDULE

16. DISTRIBUTION STATEMENT (of this Report)

Approved for public release; distribution unlimited.

17. DISTRIBUTION STATEMENT (of the abstract entered in Block 20, if different from Report)

18. SUPPLEMENTARY NOTES

19. KEY WORDS (Continue on reverse side if necessary and identify by block number)

Visibility
Vertical Structure
Atmospheric transmission
Slant path transmission
Cloud ceiling height
Haze
Fog
Stratus cloud cover

20. ABSTRACT (Continue on reverse side if necessary and identify by block number)

Based on data describing the vertical structure in haze and fog, and on empirical parameterizations of that data, an algorithm of simple analytical form has been developed that describes the vertical structure for low visibility/low ceiling conditions. The algorithm describes the vertical structure of the visible extinction coefficient and liquid water content for two regimes: (1) the case of thick fogs and low stratus clouds, where the liquid water content is governed primarily by the wet adiabatic lapse rate;

DD FORM 1 JAN 73 1473 EDITION OF 1 NOV 65 IS OBSOLETE

SECURITY CLASSIFICATION OF THIS PAGE (When Data Entered)

20. ABSTRACT (Cont)

and (2) the case of hazes and thin fogs, where the vertical structure is determined by advection, radiative and conductive cooling, and hydration processes below and at saturation.

ACKNOWLEDGMENT

The author would like to thank Mr. Robert Johnson for his help with many of the background computations. The support of Mr. Lindberg and many others at the US Army Atmospheric Sciences Laboratory who helped gather and provide the background data is gratefully acknowledged.

SUMMARY

A simple algorithm has been developed that describes the vertical structure of the visible extinction coefficient and the liquid water content (LWC) for low visibility/low ceiling conditions. The algorithm is based on a parameterization of several sets of data describing the vertical structure of hazes, fogs, and low stratus clouds. The algorithm needs as input values the value of the visible extinction coefficient $\sigma_e(0.55\mu m)$ or LWC, and the cloud ceiling height. The form of the algorithm is

$$\sigma_e \text{ or LWC} = A \exp(B \exp(Cz)) , \tag{6a}$$

where the coefficients A and B are determined by boundary values and the initial value at the surface, C determines the increase of σ_e or LWC with altitude, and z is the altitude. The visibility can be readily determined from the visible extinction coefficient or vice versa.

When the fog is so thick at the surface that the cloud ceiling height can not be determined (i.e., the sky is obscured) or one is already in the cloud, the value of the coefficient C is directly related to the increase in LWC as one rises in altitude at the wet adiabatic lapse rate and to the change in droplet size distribution associated with convective processes. When a haze or fog is present and the cloud ceiling height z_c can be determined, the coefficient C is related to the cloud ceiling height via the equation

$$C = \frac{1}{z_c} \ln\left[\frac{\ln(E/A)}{\ln(D/A)}\right] , \tag{7}$$

where A, D, and E are determined by the boundary conditions and initial values at the surface, as explained and defined in the text.

Thus, the vertical structure in visibility or LWC can be determined for low visibility/low stratus cases on the basis of two inputs: surface visibility and cloud ceiling height. The results can be extended to other wavelengths via numerous wavelength scaling laws that have been empirically derived.

The utility of this algorithm is that it relates the vertical structure to surface observations of visibility and cloud ceiling height. These latter quantities are commonly recorded in meteorological observations taken throughout the world. Therefore, frequencies or probabilities of occurrence can be determined for the vertical structure of low visibility/low ceiling conditions. The impact of these conditions on sensor and system performance can now be more readily calculated.

CONTENTS

LIST OF FIGURES

LIST OF TABLES

INTRODUCTION

The development of precision-guided munitions and sophisticated electro-optical sensors has placed new emphasis on the term visibility. Traditionally, visibility has referred to visual estimates of the range within which certain objects were discernable against the horizon. Often the visibility is measured and recorded automatically by several types of visibility meters. In either case, the emphasis has been upon the horizontal visibility. Increasingly, United States and North Atlantic Treaty Organization (NATO) military forces are relying on new surveillance and weapon systems whose sensors must function over a slant path, where variations in the vertical as well as the horizontal visibility are important.

In low visibility situations, due either to haze or fog, a growing body of observations[1-5] are showing that the measured visibility at the surface is not representative of conditions a few hundreds of meters, or even tens of meters, above the surface. Thus, "slant path visibility" can be significantly different from "horizontal visibility." In a significant fraction of the cases the visibility becomes worse as the height above the surface increases. These cases are be of special concern in this report.

Based on numerous vertical profiles of droplet size distributions, an empirical model of the vertical structure of hazes and fogs has been developed.[6] This earlier work is now extended in this report for low visibility/low stratus conditions. Two quantities of physical significance are selected: the extinction coefficient at a wavelength of 0.55μm, which directly relates to the visibility (see appendix A), and the LWC, which relates to many microphysical properties of fogs and which scales directly to

---

[1]Hoihjelle, D. L., et al, Balloon-borne Aerosol Particle Counter Measurement Mode in Wintertime at Grafenwohr, West Germany, ECOM-DR-76-3, US Army Atmospheric Sciences Laboratory, White Sands Missile Range, NM, 1976.

[2]Pinnick, R. G., et al, Vertical Structure in Atmospheric Fog and Haze and Its Effect on IR Extinction, ASL-TR-0010, US Army Atmospheric Sciences Laboratory, White Sands Missile Range, NM, 1978.

[3]Loveland, R. B., et al, Atmospheric Characterization Measurements for Copperhead Ground Fog Experiment, Internal Report, US Army Atmospheric Sciences Laboratory, White Sands Missile Range, NM, 1978.

[4]Lindberg, J. D., et al, Vertical Distribution of Fog and Haze Near Greding, Germany, During February and March 1980, Internal Report, US Army Atmospheric Sciences Laboratory, White Sands Missile Range, NM, 1980.

[5]Lindberg, J. D., Compiler, Early Wintertime European Fog and Haze: Report on Meppen 80, ASL-TR-0108, US Army Atmospheric Sciences Laboratory, White Sands Missile Range, NM, 1982.

[6]Duncan, L. D., J. D. Lindberg and R. B. Loveland, An Empirical Model of the Vertical Structure of German Fogs, ASL-TR-0071, US Army Atmospheric Sciences Laboratory, White Sands Missile Range, NM, 1980.

the extinction at many infrared wavelengths.[7] The algorithm that is developed describes the vertical structure of the extinction coefficient and LWC as a simple function of two variables: the initial value at the surface and the cloud ceiling height.

BASIS AND DERIVATION

Some detailed data on the vertical structure of fogs and hazes have been gathered in the Federal Republic of Germany (FRG) on several different occasions.[1,2,4,5] Droplet size distributions in the 0.23μm to 47μm range have been measured from a balloon-borne instrument, thus yielding vertical profiles. LWC and extinction coefficients at desired wavelengths can be calculated from these measured droplet size distributions.

The vertical structure of these profiles has been examined previously by Duncan et al,[6] who characterized the vertical structure in the form

$$y = a'x + b' , \tag{1}$$

---

[7]Pinnick, R. G., et al, Relationships Between IR Extinction, Absorption and Liquid Water Content of Fogs, ASL-TR-0037, US Army Atmospheric Sciences Laboratory, White Sands Missile Range, NM, 1979.

[1]Hoihjelle, D. L., et al, Balloon-borne Aerosol Particle Counter Measurement Mode in Wintertime at Grafenwohr, West Germany, ECOM-DR-76-3, US Army Atmospheric Sciences Laboratory, White Sands Missile Range, NM, 1976.

[2]Pinnick, R. G., et al, Vertical Structure in Atmospheric Fog and Haze and Its Effect on IR Extinction, ASL-TR-0010, US Army Atmospheric Sciences Laboratory, White Sands Missile Range, NM, 1978.

[4]Lindberg, J. D., et al, Vertical Distribution of Fog and Haze Near Greding, Germany, During February and March 1980, Internal Report, US Army Atmospheric Sciences Laboratory, White Sands Missile Range, NM, 1980.

[5]Lindberg, J. D., Compiler, Early Wintertime European Fog and Haze: Report on Meppen 80, ASL-TR-0108, US Army Atmospheric Sciences Laboratory, White Sands Missile Range, NM, 1982.

[6]Duncan, L. D., J. D. Lindberg and R. B. Loveland, An Empirical Model of the Vertical Structure of German Fogs, ASL-TR-0071, US Army Atmospheric Sciences Laboratory, White Sands Missile Range, NM, 1980.

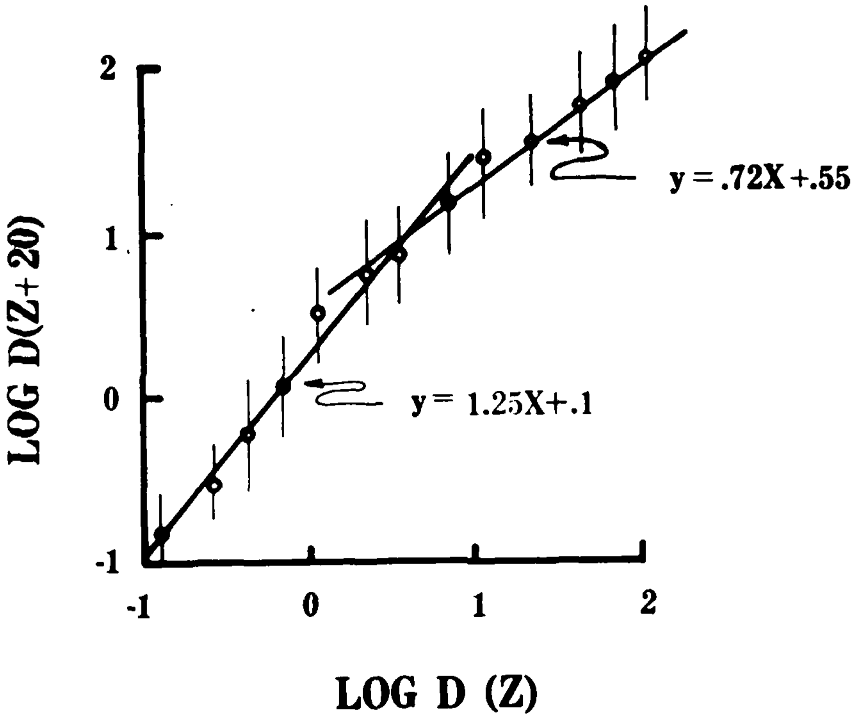

Figure 1a. Relationship between the extinction coefficient (0.55μm) at altitudes z and z + 20 m. The vertical lines are the error bars for the data (after Duncan et al[6]).

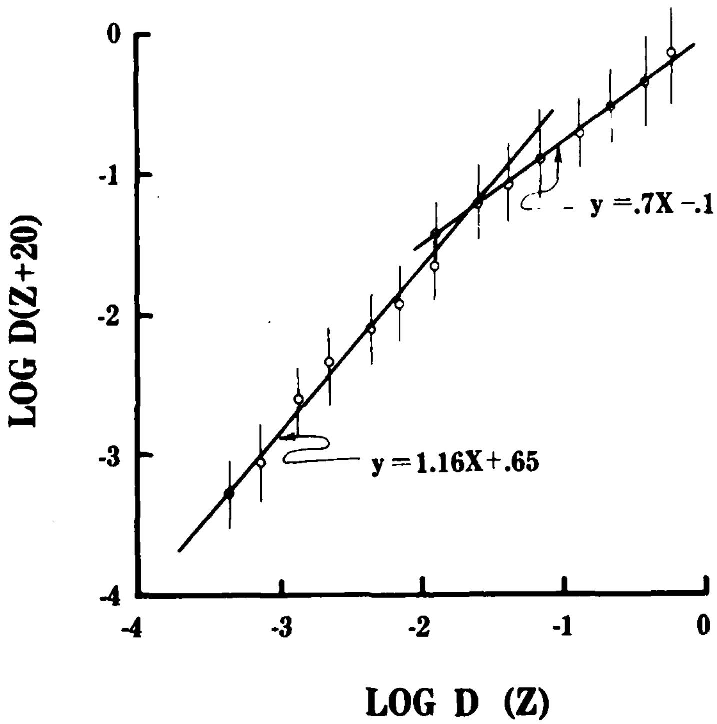

Figure 1b. Relationship between LWC at altitudes z and z + 20. The vertical lines are the error bars for the data (after Duncan et al[6]).

where $x = \log_{10}D(z)$, $y = \log_{10}D(z + 20)$, a' and b' are coefficients that were chosen to fit the data, and D(z) is the value of the desired variable (e.g. LWC) at the altitude z; D(z + 20) is then the value of this variable at an altitude of z + 20 m. Thus, one can work stepwise from the surface up through the cloud boundary layer. Figures 1a and 1b show the fits of equation (1) to the data.[6]

Two points should be noted about figures 1a and 1b before proceeding. First, each figure shows that two lines must be used to fit the data set. The point of intersection of these two lines does have physical significance, as will be shown in the next section. Second, the coefficients of the equations for the two lines have values such that there is a point at which y = x (i.e., $\log_{10}D(z + 20) = \log_{10}D(z)$). This means that there is an upper and a lower bound to the variables and their vertical profiles, or in other words there is a point where the vertical profile of σ_e or LWC no longer increases (or decreases) with altitude. Again, the physical interpretation will be discussed in the next section.

Since the variable y in equation (1) is simply the variable x(z) at an altitude of z + 20 m, the equation can be rewritten as

$$x(z + 20) - x(z) = (a' - 1)x(z) + b' . \qquad (2)$$

where x(z) has been subtracted from each side. Dividing each side by 20 m (i.e., Δz) and recognizing that x(z + 20) - x(z) is Δx, equation (2) becomes

$$\frac{\Delta x}{\Delta z} = \frac{(a' - 1)}{20} x + \frac{b'}{20} , \qquad (3)$$

which can be recast as a simple differential equation of the form

$$\frac{dx}{dz} + ax = b . \qquad (4)$$

This has a general solution of the form

$$x = (c - \frac{b}{a})e^{-az} + \frac{b}{a} , \qquad (5)$$

---

[6]Duncan, L. D., J. D. Lindberg, and R. B. Loveland, An Empirical Model of the Vertical Structure of German Fogs, ASL-TR-0071, US Army Atmospheric Sciences Laboratory, White Sands Missile Range, NM, 1980.

where c is a constant of integration determined by the boundary conditions, and a and b can be found from figures 1a and 1b and equations (1) and (3).

Since $x = \log_{10}D(z)$, the final form of the solution of the extinction coefficient ($\sigma_e(0.55\mu m)$) or LWC is

$$\sigma_e \text{ or LWC} = A \exp[B \exp(Cz)] , \tag{6a}$$

where

$$A = 10^{b/a} , \tag{6b}$$

$$B = (\ln 10)\ (c - \frac{b}{a}) , \tag{6c}$$

where ln 10 = 2.3026..., and finally

$$C = -a . \tag{6d}$$

The constant of integration c represents the $\log_{10}$ of the initial or starting value of σ_e or LWC; $\frac{b}{a}$ represents $\log_{10}$ of a bounding value for σ_e or LWC. Thus, the coefficient B may be recast in the form

$$B = \ln D - \ln A = \ln(\frac{D}{A}) , \tag{6e}$$

where D is the initial or starting value of the variable and A is the boundary value. (Note the shift to natural logarithms and exponentials.)

Tables 1a and 1b give the values of the coefficients in equation (6a) for the vertical profiles of the extinction coefficient and LWC as parameterized in figures 1a and 1b. Note that there are two equations in each figure, one for each line segment, and therefore two sets of values for each variable.

TABLE 1a. EXTINCTION COEFFICIENT

$$\sigma_e(0.55\mu m) = A \exp[B \exp(Cz)] \ (km^{-1})$$

Range of Applicability	0.398 to 7.08 km^{-1} Haze/Fog	7.08 to 92.1 km^{-1} Thick Fog/Cloud
A	0.398 km^{-1}	92.1 km^{-1}
B	ln (D/A)	ln (D/A)
C	0.0125 m^{-1}*	-0.014 m^{-1}
D	initial value	initial value

**C also may be calculated as an explicit function of cloud ceiling height; see table 2 in the next section.*

TABLE 1b. LIQUID WATER CONTENT

$$LWC = A \exp[B \exp(Cz)] \ (g/m^3)$$

Range of Applicability	8.66(-5)* to 2.34(-2) g/m^3 Haze/Fog	2.34(-2) to 4.64(-1) g/m^3 Thick Fog/Cloud
A	8.66(-5) g/m^3	4.64(-1) g/m^3
B	ln (D/A)	ln (D/A)
C	0.008 m^{-1}**	-0.015 m^{-1}
D	initial value	initial value

*8.66(-5) = 8.66×10^{-5}

**C also may be calculated as an explicit function of cloud ceiling height; see table 2 in the next section.

PHYSICAL INTERPRETATION

It is now worthwhile to examine the two sets of coefficients for equation (6a) and to determine the physical significance of the intersection of the two lines shown in figures 1a and 1b. For this purpose it is most useful to examine the algorithm for LWC. The two lines in figure 1b intersect at a value for the LWC of 0.0234 g/m^3. Analyses at the US Army Atmospheric Sciences Laboratory (ASL) of numerous vertical profiles have shown that a cloud boundary can be reasonably defined for a value of LWC between 0.02 and

0.03 g/m³. Independent analyses of numerous cases of thick fogs and clouds have also shown that 0.03 g/m³ is value representative of the boundary or transition between fog and a thick fog/cloud.[9]

The point of intersection of the two lines in figure 1b thus represents a transition between two regions of droplet growth. In the lower region, representative of hazes and fogs, the growth of droplets is governed more by aerosol hydration below and at supersaturation, radiative cooling of droplets, and heat transfer to the ground. In the upper region, representative of thick fogs and clouds, the droplet growth and hence LWC increase is governed more by convective motion. The transition takes place where LWC reaches a value in the range of 0.02 to 0.03 g/m³, which represents either a fog sufficiently dense and of sufficient vertical depth that convective cells can form,[10] or the lower boundary of a stratus cloud. The precise value of 0.0234 g/m³ is not significant in itself, but only represents an average of several sets of data.

Figure 2 shows the comparisons between LWC as a function of altitude, as calculated from equation (6a), and LWC increase due to air rising at the wet

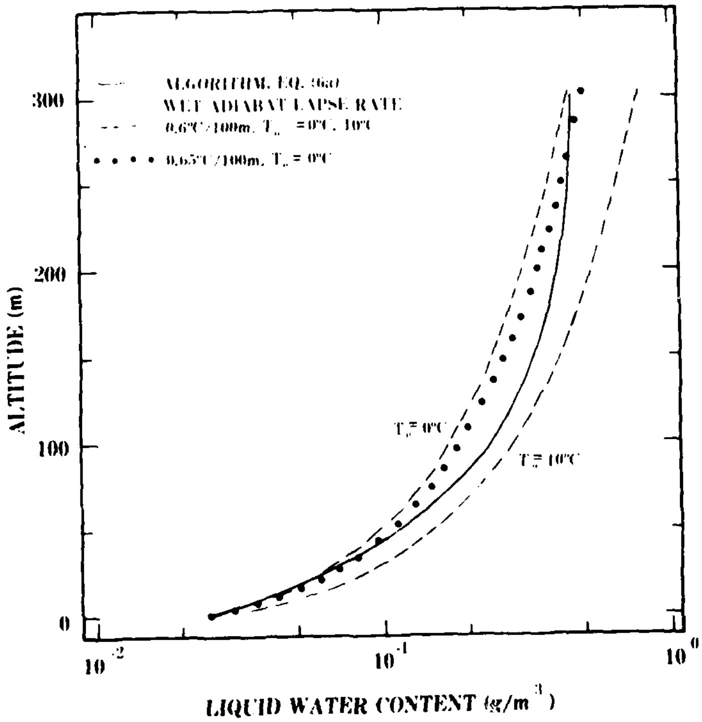

Figure 2. Comparison of LWC as determined from equation (6a) and the increase in LWC due to a parcel of air rising at the moist adiabatic lapse rate.

---

[9]Rogers, C. W., and J. T. Hanley, An Algorithm for the Increase of Liquid Water Content with Height in Fog and Water Hazes, Calspan Report No. 6711-M-1, Buffalo, NY, 1980.

adiabatic lapse rate (see appendix B). Several curves are shown for the latter case, illustrating the effects of temperature and lapse rate. The reasonable agreement between the two types of curves shows that equation (6a), with the second set of coefficients from table 1b, is an average representation of the increase in LWC due to saturated air rising at the wet adiabatic lapse rate. Physically, this means that when a fog becomes sufficiently dense, overturning motions in the fog begin,[9,10] so that further droplet growth and LWC increases are governed by convective processes and the wet adiabatic lapse rate. The presence of a cloud already indicates convective motions. Deviations from the wet adiabatic lapse rate may be expected near the earth's surface and the boundaries of the cloud.

The value of the coefficient A in equation (6a) is determined from setting y = x in figures 1a and 1b. For the upper region, this yields a value of 0.464 g/m, which is in good agreement with the fact that upper bounds to LWC in stratus clouds are on the order of 0.4 to 0.5 g/m.[11] Of course, the values can be smaller for thinner clouds that are not undergoing strong radiative cooling on top. Again, the precise value of 0.464 g/m^3 only represents an average from several sets of data. For the lower region, the boundary value is $8.66 \times 10^{-}$ g/m^3. There are two interpretations regarding the significance of this value. On the one hand, this corresponds to visibilities on the order of 7 to 10 km (light haze), which is representative of a haze aerosol that is beginning to grow as the relative humidity rises above 80 percent.[12] On the other hand, this value also represents the lower sensitivity of the instrumentation used to measure the droplet size distribution. In actuality, both effects are probably present, and this value thus represents a practical bound for the condition of lowered visibility. Once again, it is an average from several data sets.

In an analogous manner, the point of intersection of the two lines in figure 1a for the 0.55μm extinction coefficient can be related to changes in droplet size distributions. These changes are in turn due to the change in physical processes responsible for the two representations for LWC in figure 1b. Analysis of the vertical profiles of LWC and calculated extinction coefficients from the data obtained near Meppen, FRG, in 1980[5] shows that the

---

[9]Roach, W. T., et al, "The Physics of Radiation Fog: I - A Field Study," Quart J Roy Meteorol Soc, 102:313-333, 1976.

[10]Pilie, R. J., et al, "The Life Cycle of Valley Fog. Part II: Fog Microphysics," J Appl Meteorol, 14:364-374, 1975.

[11]Pruppacher, H. R., and J. D. Klett, Microphysics of Clouds and Precipitation, D. Reidel Pub Co, Dordrecht, Holland, 1978.

[12]Shettle, E. P., and R. W. Fenn, Models for the Aerosols of the Lower Atmosphere and the Effects of Humidity Variations on Their Optical Properties, AFGL-TR-79-0214, Air Force Geophysics Laboratory, Hanscomb AFB, MA, 1979.

[5]Lindberg, J. D., Compiler, Early Wintertime European Fog and Haze: Report on Meppen 80, ASL-TR-0108, US Army Atmospheric Sciences Laboratory, White Sands Missile Range, NM, 1982.

altitudes are the same for the points where σ_e equals 7.06 km^{-1} and LWC equals 0.0234 g/m^3. In a similar manner, the upper bound of 92.1 km^{-1} for σ_e represents the limiting value of transmission in a stratus cloud, while the value of 0.398 km^{-1} represents the lower limit to extinction, or the limiting value of visibility in a light haze, beyond which the algorithm should not be applied. As before, these boundary values are averages from several sets of data.

Figures 3a and 3b show plots of the vertical profiles of the extinction coefficient and LWC using equation (6a) and tables 1a and 1b. Different initial values have been selected to show the altitude dependence of the various profiles. The values of σ_e and LWC represented by the intersection points of the two lines in figure 1a and 1b are shown by dashed vertical lines. The point where the vertical profile intersects the dashed vertical lines is the nominal lower cloud boundary; the altitude is indicated in parentheses. The vertical profile up through the cloud can be obtained by adding the profile to the right of the dashed line into the profile to the left at the cloud boundary, and then extending it up to the top of the cloud.

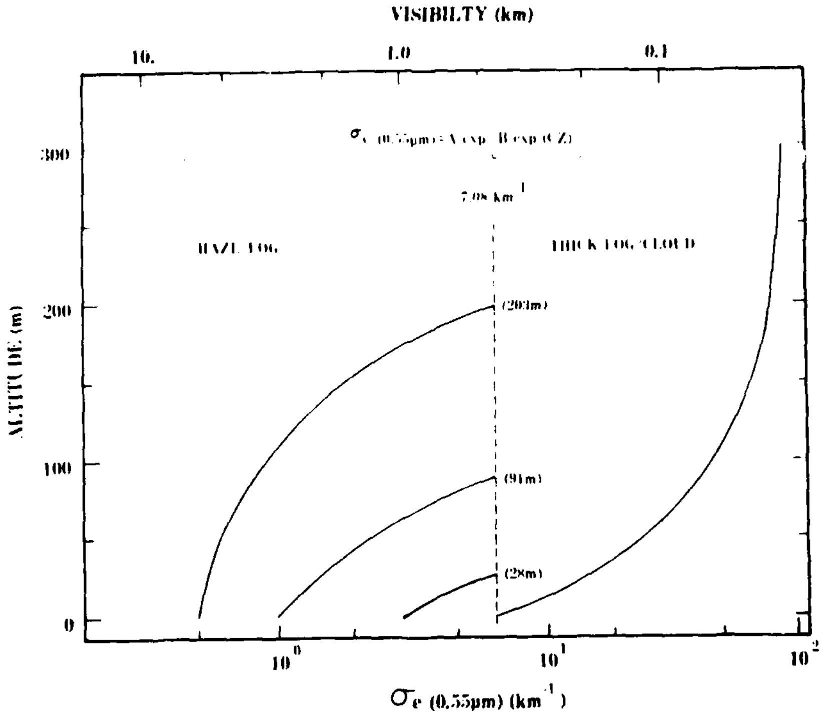

Figure 3a. The vertical profile of the 0.55μm extinction coefficient for various initial values. The profiles can be extended to the right of the dashed line by adding the profile starting at σ_e = 7.08 km^{-1} and starting at the altitude of the cloud boundary.

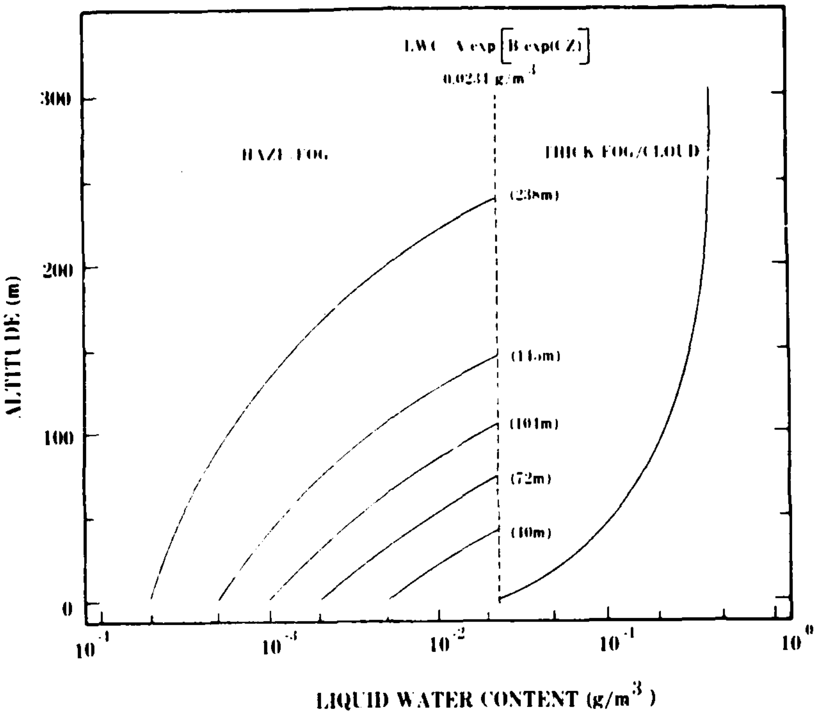

Figure 3b. The vertical profile of LWC for various initial values; similar to figure 3a.

In this current formulation, the initial value of σ_e or LWC determines the height of the lower cloud boundary. In practice, it is the cloud ceiling height and the surface value of visibility that are the observed variables. (In some rare instances LWC is also measured at the surface.) The deterministic nature of equation (6a) comes from the fact that the coefficient C is single-valued. It has been shown previously that for thick fog/cloud conditions, this value is related to the increase in LWC along a wet adiabat. For haze/fog conditions, the value of C given in tables 1a and 1b represents an average of several different haze and fog cases. Because the intersection points in figures 1a and 1b can be related to the cloud boundary, it is also possible to express the value of C as a function of the observed cloud ceiling height z_c:

$$C = \frac{1}{z_c} \ln \left[\frac{\ln (E/A)}{\ln (D/A)}\right] , \qquad (7)$$

where E is the value of the extinction coefficient or LWC at the upper bound of the range of applicability (i.e., the values of σ_e or LWC represented by

the dashed vertical lines in figures 3a and 3b) and other coefficients are defined as before. Table 2 gives the values that are appropriate in each case.

Figures 4a and 4b illustrate the cases where one initial value for σ_e and LWC has been picked, but several different ceiling heights have been specified. The solid line gives the average vertical profile from tables 1a and 1b. Thus, by the use of equations (6a) and (7), the vertical structure for low visibility/low-lying stratus conditions can be specified by the initial value at the surface and the cloud ceiling height.

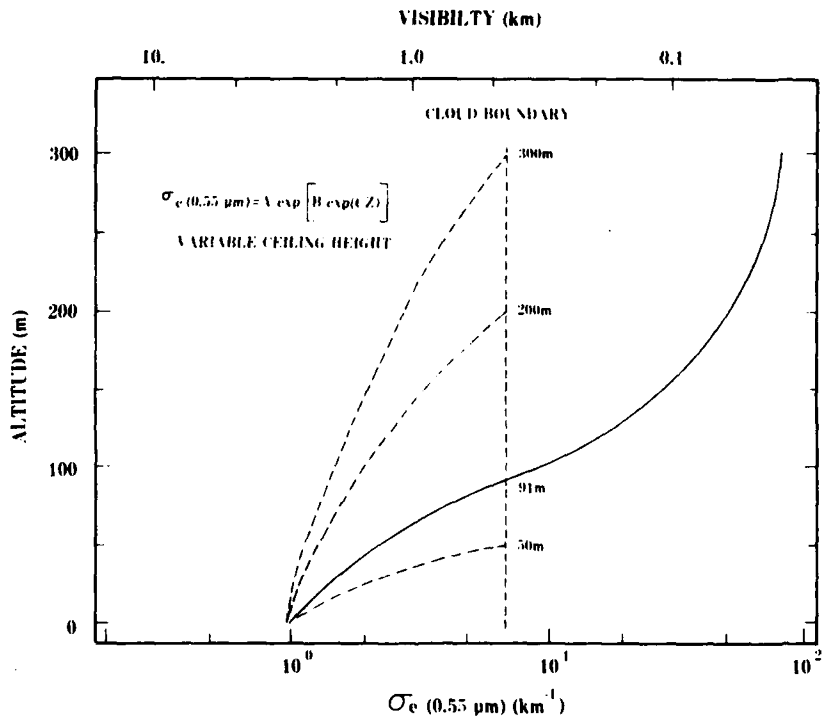

Figure 4a. The vertical profile of the 0.55μm extinction coefficient for various cloud ceiling heights. The solid line shows the averaged profile using table 1a.

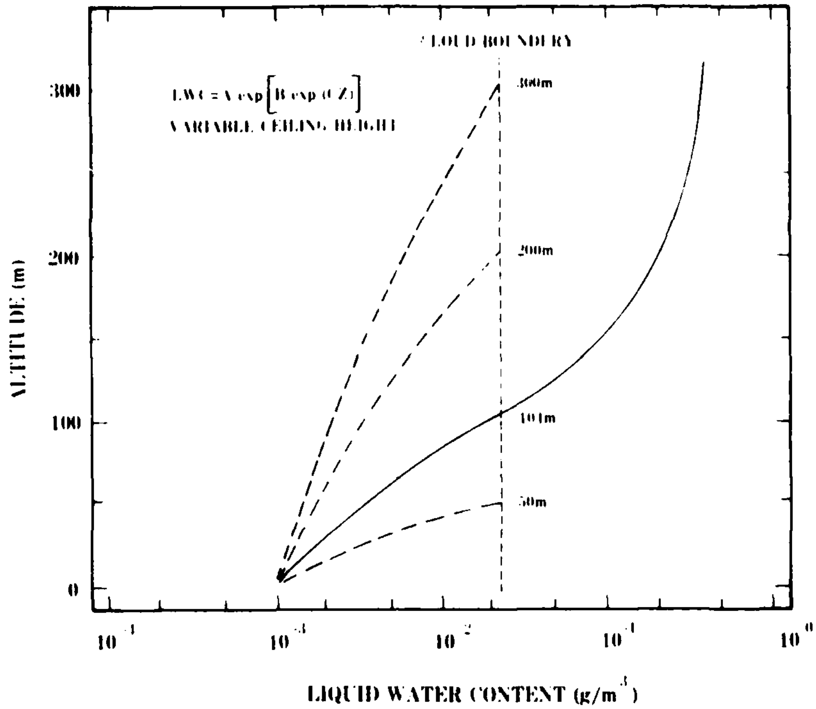

Figure 4b. The vertical profile of LWC for various cloud ceiling heights. The solid line shows the averaged profile using table 1b.

TABLE 2. COEFFICIENT C AS A FUNCTION OF CEILING HEIGHT

$$C = \frac{1}{z_c} \ln\left[\frac{\ln (E/A)}{\ln (D/A)}\right]$$

Range of Applicability	Extinction Coefficient 0.398 to 7.06 km^{-1}	Liquid Water Content 8.66(-5) to 2.34(-2) g/m^3
z_c	Cloud ceiling height (m)	Cloud ceiling height (m)
E	7.08 km^{-1}	0.0234 g/m^3
A	0.398 km^{-1}	8.66(-5) g/m^3
D	initial value	initial value

COMPARISONS WITH DATA AND EXAMPLES OF USE

The empirical representation[6] of the vertical structure shown in figures 1a and 1b was based upon the data gathered in Grafenwohr, FRG.[1, 2] A validation of the model would be to compare the algorithm based on these data with an independent set of data obtained in Meppen, FRG.[5]

Figure 5 shows the comparison between the algorithm for LWC and the data obtained from the balloon-borne particle spectrometer at Meppen. In this instance, the fog was so thick that no ceiling height could be obtained, and the initial value of LWC was greater than the dividing line value of 0.0234 g/m^3. Therefore, the right-hand column of table 1b is used to obtain the value of the constants used in equations (6a) through (6e); an initial value of 0.04 g/m^3 is estimated at the surface from the data. Substituting these values into equation (6a), one has

$$LWC = 0.464 \exp[-2.451 \exp(-0.015z)] \ . \tag{6a-1}$$

The comparison with the data in figure 5 is quite good. In general, the agreements are very good for several cases that were tested, with the values calculated by the algorithm being within ±50 percent of the data. These accuracies are within the accuracy limits that can be placed on the data itself.*

---

[6]Duncan, L. D., J. D. Lindberg and R. B. Loveland, An Empirical Model of the Vertical Structure of German Fogs. ASL-TR-0071, US Army Atmospheric Sciences Laboratory, White Sands Missile Range, NM, 1980.

[1]Hoihjelle, D. L., et al, Balloon-borne Aerosol Particle Counter Measurement Mode in Wintertime at Grafenwohr, West Germany, ECOM-DR-76-3, US Army Atmospheric Sciences Laboratory, White Sands Missile Range, NM, 1976.

[2]Pinnick, R. G., et al, Vertical Structure in Atmospheric Fog and Haze and Its Effect on IR Extinction, ASL-TR-0010, US Army Atmospheric Sciences Laboratory, White Sands Missile Range, NM, 1978.

[5]Lindberg, J. D., Compiler, Early Wintertime European Fog and Haze: Report on Meppen 80, ASL-TR-0108, US Army Atmospheric Sciences Laboratory, White Sands Missile Range, NM, 1982.

*J. D. Lindberg, private communcation.

Figure 6 shows the comparison between the algorithm and the measured LWC for a case where a cloud ceiling height can be estimated. The visibility at the surface was estimated at 3 km, with thin fog (or heavy haze) being recorded as an obstruction to vision. The cloud ceiling height was estimated from the data as the point where the dividing line value of 0.0234 g/m³ intersected the LWC profile, z_c = 150 m. (It was night when this profile was taken, and no reliable visual estimate of the cloud ceiling height could be made.) Using the right-hand column from table 2, and an estimated initial value for LWC at the surface of 0.0001 g/m³, equation (7) for C yields

$$C = \frac{1}{150\ \mathrm{m}} \ln\left[\frac{\ln(0.0234/0.0000866)}{\ln(0.0001/0.0000866)}\right] = 0.0244\ \mathrm{m}^{-1} . \qquad (7\text{-}1)$$

This value of C is now used along with the initial value at the surface in the left-hand column of table 1b to define the coefficients in equation (6a)

$$\mathrm{LWC} = 0.0000866 \exp(0.1439 \exp(0.0244z)) , \qquad (6a\text{-}2)$$

which defines the LWC profile from the surface to the lower cloud boundary. The LWC profile inside the cloud is now found by using the right-hand column of table 1b and 0.0234 g/m³ as the initial value, yielding

$$\mathrm{LWC} = 0.464 \exp[-2.987 \exp(-0.015z')] , \qquad (6a\text{-}3)$$

where z' is now the altitude above the cloud base. Again, the comparison of the calculated LWC profile with the data of figure 6 is quite reasonable; comparisons of several profiles of this type with similar cases from the ASL Meppen 80 tests likewise showed good agreement.

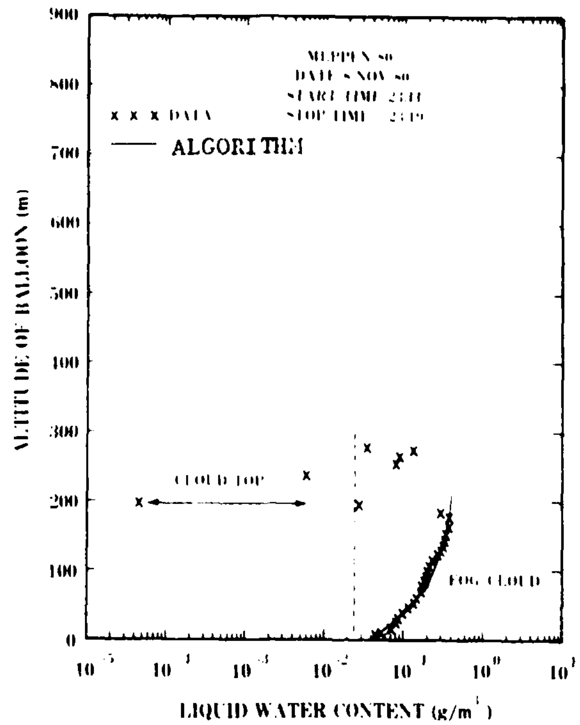

Figure 5. The comparison between the algorithm for the vertical structure of LWC and data for the case of thick fog.

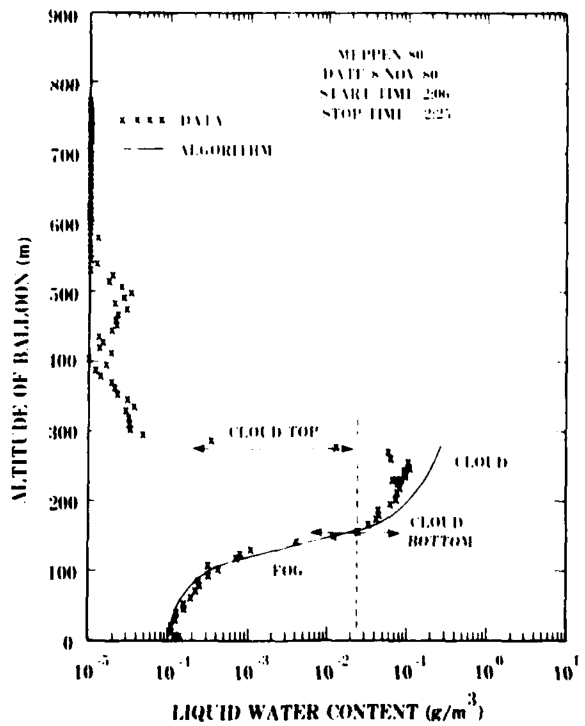

Figure 6. The comparison between the algorithm for the vertical structure of LWC and data for the case of thin fog and low stratus clouds.

Figure 7 shows the comparison of the algorithm for the visible extinction coefficient with that computed from the balloon-borne data used to calculate the LWC profile in figure 6. The estimated ceiling height is found by

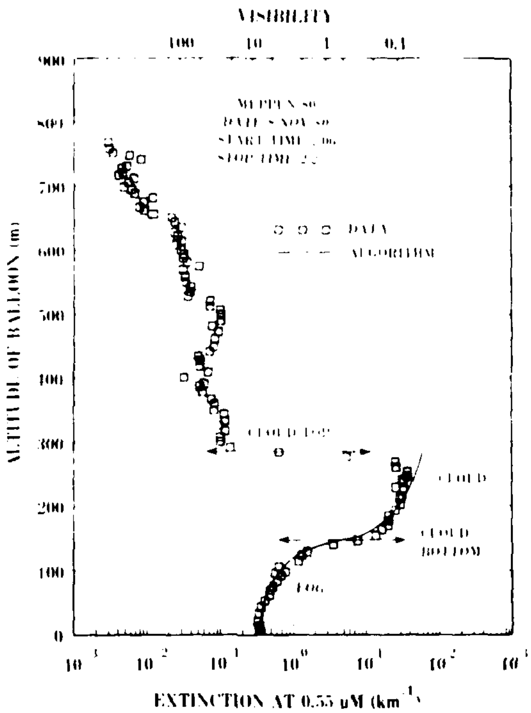

Figure 7. The comparison between the algorithm for the vertical structure of the 0.55μm extinction coefficient and data for the case of thin fog and low stratus clouds

extending the dividing line value of 7.06 km^{-1} upward until it intersects the data profile. As before, the estimated cloud ceiling height is 150 m. The value of the coefficient C is calculated by using an initial value of 0.4 km^{-1} and the coefficients from the left-hand column of table 2, yielding

$$C = \frac{1}{150\ m} \ln\left[\frac{\ln(7.06/0.398)}{\ln(0.4/0.398)}\right] = 0.0424\ m^{-1} . \tag{7-2}$$

This value of C, along with the initial value at the surface, is used in the left-hand column of table 1a to define the coefficients in equation (6a)

$$\sigma_e(0.55\mu m) = 92.1 \exp[-2.566 \exp(-0.014z')] , \tag{6a-4}$$

where z' is the altitude above the cloud base. Figure 7 shows that the comparison between the data and the algorithm is quite good.

In each of figures 5 through 7 the level of the cloud top could be determined from the data. In practice, the top boundary height of a cloud deck is usually not known, nor does the algorithm itself determine where the top of the cloud should be. Numerous examples of vertical profile data from the ASL Meppen 80 field program showed that low-lying stratus clouds have thicknesses mainly in the range of 100 to 300 m. As a rather rough average, a nominal cloud thickness of 200 m can be selected; this value allows the LWC to grow to 0.4 g/m³, which is a reasonable upper limit. Therefore, when the cloud thickness is not known, a default value of 200 m is suggested for use in the algorithm. In practice, the actual cloud thickness is not a crucial quantity. The attenuation at the cloud base increases so rapidly with increasing altitude that after the first 50 to 100 m of cloud thickness, essentially no transmission in either the visible or infrared occurs.

DISCUSSION AND CONCLUSIONS

The preceding sections describe a simple algorithm that has been developed to describe the vertical structure of the visible extinction coefficient and LWC for low visibility/low ceiling conditions. The visible extinction coefficient has been selected because of its direct relationship to visibility, which is a commonly observed and recorded meteorological quantity, and because of the numerous existing scaling laws that relate the visible extinction coefficient to the desired infrared extinction coefficient. LWC has been selected because of its relation to many fog and cloud microphysical properties and because it directly scales to the extinction or absorption coefficients at several infrared wavelengths.

The algorithm is applicable in cases of lowered visibility (< 7 km) and low or obscured ceilings. The algorithm has two sets of coefficients, each set applicable to a different regime. The first regime is for hazes and fogs, where the visibility ranges from 7 km down to approximately 0.4 km, and a low cloud ceiling is present. In this regime the algorithm needs as input values the visible extinction coefficient or LWC, and the cloud ceiling height. The second regime is for thick fogs (visibility < 0.4 km), where the sky is obscured, or when one is already in the cloud. Here the input parameter is either the visible extinction coefficient or LWC; appropriate boundary values have been determined from the data. Because the depth of thick fog and the vertical thickness of low-lying stratus clouds are not easily obtainable quantities, a default value of 200 m is suggested when this information is not otherwise available.

The algorithm should not be used when the visibility is greater than 7 km, when there is no cloud ceiling, or when the cloud ceiling is above 1 km. There is such a paucity of data for these cases than an extension to these regimes is not currently warranted. As more information on the vertical distributions of aerosols in the planetary boundary layer and the visibility vertical structure becomes available, these difficulties will be overcome.

The vertical profiles used to develop this algorithm are from tethered balloon flights, all of which are for altitudes of less than 800 m (above the launch site). There is a lack of data to determine what the upper bound on ceiling

heights should be. It is recommended that if the cloud ceiling height is above 1000 m (i.e., nominally above the planetary boundary layer), then the algorithm should not be used.

The case of surface haze layers and shallow radiation fogs, which can significantly reduce horizontal visibility, is being studied further at ASL. In this case, a cloud ceiling is usually not present, and the visibility improves rather than degrades with increasing altitude. While the overall frequency of occurrence of this type of vertical structure is probably larger than that for the case where the algorithm is applicable, the impact on certain types of system performance is less, because the transmittance along the air-to-surface slant path is greater than along the equivalent horizontal surface path. Current research and data-gathering efforts are being carried out at ASL to develop an algorithm for this type of vertical structure.

In summary, an algorithm of simple analytical form has been developed, which describes the vertical structure for low visibility/low ceiling conditions. The utility of this algorithm is that it relates the vertical structure to surface observations of visibility and cloud ceiling height. These latter quantities are commonly recorded in meteorological observations taken throughout the world. The visible extinction coefficient and LWC have been used as parameters for the algorithm. The visibility itself or extinction coefficients at other wavelengths could have been used just as well. Appendix C provides a succinct set of tables of coefficients for the algorithm for the parameters of visibility, 0.55μm, 4.0μm, and 10.6μm extinction coefficients, and LWC.

REFERENCES

1. Hoihjelle, D. L., et al, Balloon-borne Aerosol Particle Counter Measurement Mode in Wintertime at Grafenwohr, West Germany, ECOM-DR-76-3, US Army Atmospheric Sciences Laboratory, White Sands Missile Range, NM, 1976.

2. Pinnick, R. G., et al, Vertical Structure in Atmospheric Fog and Haze and Its Effect on IR Extinction, ASL-TR-0010, US Army Atmospheric Sciences Laboratory, White Sands Missile Range, NM, 1978.

3. Loveland, R. B., et al, Atmospheric Characterization Measurements for Copperhead Ground Fog Experiment, Internal Report, US Army Atmospheric Sciences Laboratory, White Sands Missile Range, NM, 1978.

4. Lindberg, J. D., et al, Vertical Distribution of Fog and Haze Near Greding, Germany, During February and March 1980, Internal Report, US Army Atmospheric Sciences Laboratory, White Sands Missile Range, NM, 1980.

5. Lindberg, J. D., Compiler, Early Wintertime European Fog and Haze: Report on Meppen 80, ASL-TR-0108, US Army Atmospheric Sciences Laboratory, White Sands Missile Range, NM, 1982.

6. Duncan, L. D., J. D. Lindberg and R. B. Loveland, An Empirical Model of the Vertical Structure of German Fogs, ASL-TR-0071, US Army Atmospheric Sciences Laboratory, White Sands Missile Range, NM, 1980.

7. Pinnick, R. G., et al, Relationships Between IR Extinction, Absorption and Liquid Water Content of Fogs, ASL-TR-0037, US Army Atmospheric Sciences Laboratory, White Sands Missile Range, NM, 1979.

8. Rogers, C. W., and J. T. Hanley, An Algorithm for the Increase of Liquid Water Content with Height in Fog and Water Hazes, Calspan Report No. 6711-M-1, Buffalo, NY, 1980.

9. Roach, W. T., et al, "The Physics of Radiation Fog: I - A Field Study," Quart J Roy Meteorol Soc, 102:313-333, 1976.

10. Pilie, R. J., et al, "The Life Cycle of Valley Fog. Part II: Fog Microphysics," J Appl Meteorol, 14:364-374, 1975.

11. Pruppacher, H. R., and J. D. Klett, Microphysics of Clouds and Precipitation, D. Reidel Pub Co, Dordrecht, Holland, 1978.

12. Shettle, E. P. and R. W. Fenn, Models for the Aerosols of the Lower Atmosphere and the Effects of Humidity Variations on Their Optical Properties, AFGL-TR-79-0214, Air Force Geophysics Laboratory, Hanscomb AFB, MA, 1979.

APPENDIX A

VISIBILITY DEFINITION

A brief statement on the use of the term "visibility" is in order. Three terms are commonly used: visibility, visual range, and meteorological range. The latter two have precise definitions,[1] although all three are often used interchangeably. The visual range, R_v, may be defined as

$$R_v = \frac{1}{\sigma_e} \ln \frac{C}{\varepsilon}, \qquad \text{(A-1)}$$

where σ_e is the extinction coefficient in the visual wavelength band, C is the inherent contrast of the target against the background, and ε is the threshold contrast of the observer. The meteorological range, R_m, is defined as above for the case where a black target is against the background, so that C=1, and where the visual contrast threshold is taken as ε=0.02, a near-optimum value for daylight conditions. Thus,

$$R_m = \frac{1}{\sigma_e} \ln \frac{1}{0.02} = \frac{3.912}{\sigma_e}. \qquad \text{(A-2)}$$

The meteorological range is often taken as the "visibility," but it should be clear that this is an optimum visibility.

In practice, the visual range is a more useful quantity because it allows for a target/background contrast of less than unity and/or a threshold contrast of more than 2 percent. Many visibility meters are calibrated on the basis of an assumed "observer" threshold contrast of 5 percent (or a combination of target contrast and perceptual threshold contrast so that $C/\varepsilon = \frac{1}{0.05}$). The visual range would be

$$R_v = \frac{1}{\sigma_e} \ln \frac{1}{0.05} = \frac{3.00}{\sigma_e}. \qquad \text{(A-3)}$$

The visual range defined in this manner is a slightly more conservative estimate than the meteorological range (R_v = 0.766 R_m), but it correlates better with the visibility reported in meteorological observations.[2] The term

---

[1]McCartney, E. J., <u>Optics of the Atmosphere</u>, John Wiley and Sons, Inc., New York, 1976.

"visibility" in the text is used in this sense of visual range. Conversions from extinction coefficient to visibility, such as in figures 3a, 4a, and 7, were made using equation (A-3).

---

[2]Gordon, J. I., Daytime Visibility: A Conceptual Review, AFGL-TR-79-0257, Air Force Geophysics Laboratory, Hanscomb AFB, MA, 1979.

APPENDIX B

COMPUTATION OF LIQUID WATER CONTENTS AND LIQUID WATER CONTENT LAPSE RATES FOR MOIST ADIABATIC PROCESSES

LWC and its lapse rates were obtained by computing the change in the water vapor saturation mixing ratio (ΔR_s) over a specified height interval (10 m) and then converting that change to LWC and $\Delta LWC/\Delta Z$. The equations used were

$$T(Z) = T_o - \gamma_w Z \tag{B-1}$$

$$P(Z) = P_o \left(\frac{T(Z)}{T_o}\right)^{\left(\frac{g}{R\gamma_w}\right)} \quad (P_o \text{ in mbar}) \tag{B-2}$$

$$e_s(Z) = (6.11 \text{ mbar}) \exp \left[\frac{m_v L}{R^*} \left(\frac{1}{273.15} - \frac{1}{T(Z)}\right)\right] \tag{B-3}$$

$$R_s(Z) = .622 \left(\frac{e_s(Z)}{P(Z) - e_s(Z)}\right) \tag{B-4}$$

$$\Delta R_s = (R_s)_o - R_s(Z) \tag{B-5}$$

$$\rho_a(Z) = 1/2\left(\frac{P(Z)}{T(Z)R} + \frac{P_o}{T_o R}\right) \times (100) \quad \text{(100 is a conversion factor for the mixture of units used here)} \tag{B-6}$$

$$\Delta LWC = \rho_a \, \Delta R_s \; (g/m^3) \tag{B-7}$$

$$LWC = \Delta(LWC) + LWC_o \tag{B-8}$$

$$\Delta LWC/\Delta Z = \frac{\Delta(LWC)}{\Delta Z} \tag{B-9}$$

where R_s = water vapor saturation mixing ratio

Z = height (meters)

T = absolute temperature (degrees Kelvin)

γ_w = moist adiabatic lapse rate ($\sim$ 0.6°C/100 m)

g = gravitational acceleration 9.806 m s^{-2}

R = gas constant for air 2.8704 x 10^{-1} J/g K

e_s = saturation vapor pressure for water (millibars)

L = latent heat of condensation 2.485 x 10^3 J/g

R* = universal gas constant 8.3144 J/K mol

m_v = molecular weight of water vapor 18.016 g mol^{-1}

ρ_a = air density (1,275 g/m³ at P_o = 1000 mbar and T_o = 0°C

$(\ )_o$ = values at the initial reference level (i.e., P_o = 1000 mbar and selected T_o, LWC_o = 0.0234 g/m³), or values at the previous reference level.

APPENDIX C

TABULARIZED ALGORITHM COEFFICIENTS

This appendix contains the tables of coefficients for the vertical structure algorithm. The derivations for the 0.55μm extinction coefficient and the LWC are given in the text. The tabularized values for the visibility are taken directly from the 0.55μm extinction coefficient via the relationship (see also appendix A)

$$\text{Vis} = \frac{3.0}{\sigma_e(0.55\mu m)} \quad . \tag{C-1}$$

The tabularized values for the 4.0μm and 10.6μm extinction coefficients are derived from the parametrized data in an earlier report by Duncan and associates.[1]

---

[1]Duncan, L. D., J. D. Lindberg and R. B. Loveland, An Empirical Model of the Vertical Structure of German Fogs, ASL-TR-0071, US Army Atmospheric Sciences Laboratory, White Sands Missile Range, NM, 1980.

TABLE C-1. VISIBILITY (Vis)

$$Vis = A \exp[B \exp(Cz)]$$

Range of Applicability	7.5 to 0.42 km Haze/Fog	0.42 to 0.03 km Thick Fog/Cloud
A	7.54 km	0.0326 km
B	$\ln(D/A)$	$\ln(D/A)$
C	$\frac{1}{z_c} \ln[\frac{\ln(E/A)}{\ln(D/A)}]$	$-0.014\ m^{-1}$
D	visibility at surface	visibility at surface (or at cloud boundary: 0.425 km)
E	0.425 km	(not used)
z_c	cloud ceiling height[1] (meters)	(not used)[2]

[1]If the cloud ceiling height is greater than 1 km, the algorithm should probably not be used.

[2]If the height of the fog top or the cloud thickness is not known, assign a default value of 200 m and use this portion of the algorithm only over that interval.

TABLE C-2. 0.55μm EXTINCTION COEFFICIENT

$$\sigma_e(0.55\mu m) = A \exp[B \exp(Cz)]$$

Range of Applicability	0.398 to 7.08 km^{-1} Haze/Fog	7.08 to 92.1 km^{-1} Thick Fog/Cloud
A	0.398 km^{-1}	92.1 km^{-1}
B	ln(D/A)	ln(D/A)
C	$\frac{1}{z_c} \ln[\frac{\ln(E/A)}{\ln(D/A)}]$	-0.014 m^{-1}
D	initial value at surface	initial value at surface (or at cloud boundary: 7.08 km^{-1}
E	7.08 km^{-1}	(not used)
z_c	cloud ceiling height[1] (meters)	(not used)[2]

[1]If the cloud ceiling height is greater than 1 km, the algorithm should probably not be used.

[2]If the height of the fog top or the cloud thickness is not known, assign a default value of 200 m and use this portion of the algorithm only over that interval.

TABLE C-3. 4.0μm EXTINCTION COEFFICIENT

$\sigma_e(4.0\mu m) = A \exp[B \exp(Cz)]$

Range of Applicability	3.16(-2)* to 3.32 km^{-1} Haze/Fog	3.32 to 92.1 km^{-1} Thick Fog/Cloud
A	3.16(-2) km^{-1}	92.1 km^{-1}
B	ln(D/A)	ln(D/A)
C	$\frac{1}{Z_C} \ln[\frac{\ln(E/A)}{\ln(D/A)}]$	-0.014 m^{-1}
D	initial value at surface	initial value at surface (or at cloud boundary: 3.32 km^{-1}
E	3.32 km^{-1}	(not used)
Z_C	cloud ceiling height[1] (meters)	(not used)[2]

*3.16(-2) = 3.16 x 10^{-2}

[1]If the cloud ceiling height is greater than 1 km, the algorithm should probably not be used.

[2]If the height of the fog top or the cloud thickness is not known, assign a default value of 200 m and use this portion of the algorithm only over that interval.

TABLE C-4. 10.6μm EXTINCTION COEFFICIENT

$\sigma_e(10.6\mu m) = A \exp[B \exp(Cz)]$

Range of Applicability	$1.0(-2)^*$ to 1.67 km^{-1} Haze/Fog	1.67 to 100 km^{-1} Thick Fog/Cloud
A	0.01 km^{-1}	100 km^{-1}
B	$\ln(D/A)$	$\ln(D/A)$
C	$\frac{1}{z_c} \ln[\frac{\ln(E/A)}{\ln(D/A)}]$	0.0125 m^{-1}
D	initial value at surface	initial value at surface (or at cloud boundary: 1.67 km^{-1})
E	1.67 km^{-1}	(not used)
z_c	cloud ceiling height[1] (meters)	(not used)[2]

$^*1.0(-2) = 1.0 \times 10^{-2}$

[1]If the cloud ceiling height is greater than 1 km, the algorithm should probably not be used.

[2]If the height for the fog top or the cloud thickness is not known, assign a default value of 200 m and use this portion of the algorithm only over that interval.

TABLE C-5. LIQUID WATER CONTENT

$$LWC = A \exp[B \exp(Cz)]$$

Range of Applicability	8.66(-5)* to 2.34(-2) g/m^3 Haze/Fog	2.34(-2) to 4.64(-1) g/m^3 Thick Fog/Cloud
A	8.66(-5) g/m^3	4.64(-1) g/m^3
B	ln(D/A)	ln(D/A)
C	$\frac{1}{z_c} \ln[\frac{\ln(E/A)}{\ln(D/A)}]$	$-0.15\ m^{-1}$
D	initial value at surface	initial value at surface (or at cloud boundary: 2.34(-2) g/m^3)
E	2.34(-2) g/m^3	(not used)
z_c	cloud ceiling height[1] (meters)	(not used)[2]

*8.66(-5) = 8.66×10^{-5}

[1]If the cloud ceiling height is greater than 1 km, the algorithm should probably not be used.

[2]If the height of the fog top or the cloud thickness is not known, assign a default value of 200 m and use this portion of the algorithm only over that interval.

ELECTRO-OPTICS DISTRIBUTION LIST

Commander
US Army Aviation School
Fort Rucker, AL 36362

Commander
US Army Aviation Center
ATTN: ATZQ-D-MA (Mr. Oliver N. Heath)
Fort Rucker, AL 36362

Commander
US Army Aviation Center
ATTN: ATZQ-D-MS (Mr. Donald Wagner)
Fort Rucker, AL 36362

NASA/Marshall Space Flight Center
ATTN: ES-83 (Otha H. Vaughan, Jr.)
Huntsville, AL 35812

NASA/Marshall Space Flight Center
Atmospheric Sciences Division
ATTN: Code ES-81 (Dr. William W. Vaughan)
Huntsville, AL 35812

Nichols Research Corporation
ATTN: Dr. Lary W. Pinkley
4040 South Memorial Parkway
Huntsville, AL 35802

John M. Hobbie
c/o Kentron International
2003 Byrd Spring Road
Huntsville, AL 35802

Mr. Ray Baker
Lockheed-Missile & Space Company
4800 Bradford Blvd
Huntsville, AL 35807

Commander
US Army Missile Command
ATTN: DRSMI-OG (Mr. Donald R. Peterson)
Redstone Arsenal, AL 35809

Commander
US Army Missile Command
ATTN: DRSMI-OGA (Dr. Bruce W. Fowler)
Redstone Arsenal, AL 35809

Commander
US Army Missile Command
ATTN: DRSMI-REL (Dr. George Emmons)
Redstone Arsenal, AL 35809

Commander
US Army Missile Command
ATTN: DRSMI-REO (Huey F. Anderson)
Redstone Arsenal, AL 35809

Commander
US Army Missile Command
ATTN: DRSMI-REO (Mr. Maxwell W. Harper)
Redstone Arsenal, AL 35809

Commander
US Army Missile Command
ATTN: DRSMI-REO (Mr. Gene Widenhofer)
Redstone Arsenal, AL 35809

Commander
US Army Missile Command
ATTN: DRSMI-RHC (Dr. Julius Q. Lilly)
Redstone Arsenal, AL 35809

Commander
US Army Missile Command
Redstone Scientific Information Center
ATTN: DRSMI-RPRD (Documents Section)
Redstone Arsenal, AL 35809

Commander
US Army Missile Command
ATTN: DRSMI-RRA (Dr. Oskar Essenwanger)
Redstone Arsenal, AL 35809

Commander
US Army Missile Command
ATTN: DRSMI-RRO (Mr. Charles Christensen)
Redstone Arsenal, AL 35809

Commander
US Army Missile Command
ATTN: DRSMI-RPO (Dr. George A. Tanton)
Redstone Arsenal, AL 35809

Commander
US Army Communications Command
ATTN: CC-OPS-PP
Fort Huachuca, AZ 85613

Commander
US Army Intelligence Center & School
ATTN: ATSI-CD-CS (Mr. Richard G. Cundy)
Fort Huachuca, AZ 85613

Commander
US Army Intelligence Center & School
ATTN: ATSI-CD-MD (Mr. Harry Wilder)
Fort Huachuca, AZ 85613

Commander
US Army Intelligence Center & School
ATTN: ATSI-CS-C (2LT Coffman)
Fort Huachuca, AZ 85613

Commander
US Army Yuma Proving Ground
ATTN: STEYP-MSA-TL
Bldg 2105
Yuma, AZ 85364

Northrop Corporation
Electro-Mechanical Division
ATTN: Dr. Richard D. Tooley
500 East Orangethorpe Avenue
Anaheim, CA 92801

Commander
Naval Weapons Center
ATTN: Code 3918 (Dr. Alexis Shlanta)
China Lake, CA 93555

Hughes Helicopters
Army Advanced Attack Helicopter Weapons
ATTN: Mr. Charles R. Hill
Centinela and Teale Streets
Bldg 305, MS T-73A
Culter City, CA 90230

Commander
US Army Combat Developments
Experimentation Command
ATTN: ATEC-PL-M (Mr. Gary G. Love)
Fort Ord, CA 93941

SRI International
ATTN: K2060/Dr. Edward E. Uthe
333 Ravenswood Avenue
Menlo Park, CA 94025

SRI International
ATTN: Mr. J. E. Van der Laan
333 Ravenswood Avenue
Menlo Park, CA 94025

Joane May
Naval Environmental Prediction
Research Facility (NEPRF)
ATTN: Library
Monterey, CA 93940

Sylvania Systems Group,
Western Division
GTE Products Corporation
ATTN: Technical Reports Library
P.O. Box 205
Mountain View, CA 94042

Sylvania Systems Group
Western Division
GTE Products Corporation
ATTN: Mr. Lee W. Carrier
P.O. Box 188
Mountain View, CA 94042

Pacific Missile Test Center
Geophysics Division
ATTN: Code 3250-3 (R. de Violini)
Point Mugu, CA 93042

Pacific Missile Test Center
Geophysics Division
ATTN: Code 3253 (Terry E. Battalino)
Point Mugu, CA 93042

Effects Technology Inc.
ATTN: Mr. John D. Carlyle
5383 Hollister Avenue
Santa Barbara, CA 93111

Commander
Naval Ocean Systems Center
ATTN: Code 532 (Dr. Juergen Richter)
San Diego, CA 92152

Commander
Naval Ocean Systems Center
ATTN: Code 5322 (Mr. Herbert G. Hughes)
San Diego, CA 92152

Commander
Naval Ocean Systems Center
ATTN: Code 4473 (Tech Library)
San Diego, CA 92152

The RAND Corporation
ATTN: Ralph Huschke
1700 Main Street
Santa Monica, CA 90406

Particle Measuring Systems, Inc.
ATTN: Dr. Robert G. Knollenberg
1855 South 57th Court
Boulder, CO 80301

US Department of Commerce
National Oceanic and Atmospheric Admin
Environmental Research Laboratories
ATTN: Library, R-51, Technical Reports
325 Broadway
Boulder, CO 80303

US Department of Commerce
National Oceanic and Atmospheric Admin
Environmental Research Laboratories
ATTN: R45X3 (Dr. Vernon E. Derr)
Boulder, CO 80303

US Department of Commerce
National Telecommunications and
Information Administration
Institute for Telecommunication Sciences
ATTN: Code 1-3426 (Dr. Hans J. Liebe)
Boulder, CO 80303

AFATL/DLODL
Technical Library
Eglin AFB, FL 32542

Commanding Officer
Naval Training Equipment Center
ATTN: Technical Information Center
Orlando, FL 32813

Georgia Institute of Technology
Engineering Experiment Station
ATTN: Dr. Robert W. McMillan
Atlanta, GA 30332

Georgia Institute of Technology
Engineering Experiment Station
ATTN: Dr. James C. Wiltse
Atlanta, GA 30332

Commandant
US Army Infantry Center
ATTN: ATSH-CD-MS-E (Mr. Robert McKenna)
Fort Benning, GA 31805

Commander
US Army Signal Center & Fort Gordon
ATTN: ATZHCD-CS
Fort Gordon, GA 30905

Commander
US Army Signal Center & Fort Gordon
ATTN: ATZHCD-O
Fort Gordon, GA 30905

USAFETAC/DNE
ATTN: Mr. Charles Glauber
Scott AFB, IL 62225

Commander
Air Weather Service
ATTN: AWS/DNDP (LTC Kit G. Cottrell)
Scott AFB, IL 62225

Commander
Air Weather Service
ATTN: AWS/DOOF (MAJ Robert Wright)
Scott AFB, IL 62225

Commander
US Army Combined Arms Center
& Ft. Leavenworth
ATTN: ATZLCA-CAA-Q (Mr. H. Kent Pickett)
Fort Leavenworth, KS 66027

Commander
US Army Combined Arms Center
& Ft. Leavenworth
ATTN: ATZLCA-SAN (Robert DeKinder, Jr.)
Fort Leavenworth, KS 66027

Commander
US Army Combined Arms Center
& Ft. Leavenworth
ATTN: ATZLCA-SAN (Mr. Kent I. Johnson)
Fort Leavenworth, KS 66027

Commander
US Army Combined Arms Center
& Ft. Leavenworth
ATTN: ATZLCA-WE (LTC Darrell Holland)
Fort Leavenworth, KS 66027

President
USAARENBD
ATTN: ATZK-AE-TA (Dr. Charles R. Leake)
Fort Knox, KY 40121

Commander
US Army Armor Center and Fort Knox
ATTN: ATZK-CD-MS
Fort Knox, KY 40121

Commander
US Army Armor Center and Fort Knox
ATTN: ATZK-CD-SD
Fort Knox, KY 40121

Aerodyne Research Inc.
ATTN: Dr. John F. Ebersole
Crosby Drive
Bedford, MA 01730

Commander
Air Force Geophysics Laboratory
ATTN: OPA (Dr. Robert W. Fenn)
Hanscom AFB, MA 01731

Commander
Air Force Geophysics Laboratory
ATTN: OPI (Dr. Robert A. McClatchey)
Hanscom AFB, MA 01731

Massachusetts Institute of Technology
Lincoln Laboratory
ATTN: Dr. T. J. Goblick, B-370
P.O. Box 73
Lexington, MA 02173

Massachusetts Institute of Technology
Lincoln Laboratory
ATTN: Dr. Michael Gruber
P.O. Box 73
Lexington, MA 02173

Raytheon Company
Equipment Division
ATTN: Dr. Charles M. Sonnenschein
430 Boston Post Road
Wayland, MA 01778

Commander
US Army Ballistic Research Laboratory/
ARRADCOM
ATTN: DRDAR-BLB (Mr. Richard McGee)
Aberdeen Proving Ground, MD 21005

Commander/Director
Chemical Systems Laboratory
US Army Armament Research
& Development Command
ATTN: DRDAR-CLB-PS (Dr. Edward Stuebing)
Aberdeen Proving Ground, MD 21010

Commander/Director
Chemical Systems Laboratory
US Army Armament Research
& Development Command
ATTN: DRDAR-CLB-PS (Mr. Joseph Vervier)
Aberdeen Proving Ground, MD 21010

Commander/Director
Chemical Systems Laboratory
US Army Armament Research
& Development Command
ATTN: DRDAR-CLY-A (Mr. Ronnald Pennsyle)
Aberdeen Proving Ground, MD 21010

Commander
US Army Ballistic Research Laboratory/
ARRADCOM
ATTN: DRDAR-TSB-S (STINFO)
Aberdeen Proving Ground, MD 21005

Commander
US Army Electronics Research
& Development Command
ATTN: DRDEL-CCM (W. H. Pepper)
Adelphi, MD 20783

Commander
US Army Electronics Research
& Development Command
ATTN: DRDEL-CG/DRDEL-DC/DRDEL-CS
2800 Powder Mill Road
Adelphi, MD 20783

Commander
US Army Electronics Research
& Development Command
ATTN: DRDEL-CT
2800 Powder Mill Road
Adelphi, MD 20783

Commander
US Army Electronics Research
& Development Command
ATTN: DRDEL-PAO (M. Singleton)
2800 Powder Mill Road
Adelphi, MD 20783

Project Manager
Smoke/Obscurants
ATTN: DRDPM-SMK
(Dr. Anthony Van de Wal, Jr.)
Aberdeen Proving Ground, MD 21005

Project Manager
Smoke/Obscurants
ATTN: DRDPM-SMK-T (Mr. Sidney Gerard)
Aberdeen Proving Ground, MD 21005

Commander
US Army Test & Evaluation Command
ATTN: DRSTE-AD-M (Mr. Warren M. Baity)
Aberdeen Proving Ground, MD 21005

Commander
US Army Test & Evaluation Command
ATTN: DRSTE-AD-M (Dr. Norman E. Pentz)
Aberdeen Proving Ground, MD 21005

Director
US Army Materiel Systems Analysis Activity
ATTN: DRXSY-AAM (Mr. William Smith)
Aberdeen Proving Ground, MD 21005

Director
US Army Materiel Systems Analysis Activity
ATTN: DRXSY-CS (Mr. Philip H. Beavers)
Aberdeen Proving Ground, MD 21005

Director
US Army Materiel Systems Analysis Activity
ATTN: DRXSY-GB (Wilbur L. Warfield)
Aberdeen Proving Ground, MD 21005

Director
US Army Materiel Systems Analysis Activity
ATTN: DRXSY-GP (Mr. Fred Campbell)
Aberdeen Proving Ground, MD 21005

Director
US Army Material Systems Analysis Activity
ATTN: DRXSY-GP (H. Stamper)
Aberdeen Proving Grounds, MD 21005

Director
US Army Materiel Systems Analysis Activity
ATTN: DRXSY-GS
(Mr. Michael Starks/Mr. Julian Chernick)
Aberdeen Proving Ground, MD 21005

Director
US Army Materiel Systems Analysis Activity
ATTN: DRXSY-J (Mr James F. O'Bryon)
Aberdeen Proving Ground, MD 21005

Director
US Army Materiel Systems Analysis Activity
ATTN: DRXSY-LM (Mr. Robert M. Marchetti)
Aberdeen Proving Ground, MD 21005

Commander
Harry Diamond Laboratories
ATTN: Dr. William W. Carter
2800 Powder Mill Road
Adelphi, MD 20783

Commander
Harry Diamond Laboratories
ATTN: DELHD-R-CM (Mr. Robert McCoskey)
2800 Powder Mill Road
Adelphi, MD 20783

Commander
Harry Diamond Laboratories
ATTN: DELHD-R-CM-NM (Dr. Robert Humphrey)
2800 Powder Mill Road
Adelphi, MD 20783

Commander
Harry Diamond Laboratories
ATTN: DELHD-R-CM-NM (Dr. Z. G. Sztankay)
2800 Powder Mill Road
Adelphi, MD 20783

Commander
Harry Diamond Laboratories
ATTN: DELHD-R-CM-NM (Dr. Joseph Nemarich)
2800 Powder Mill Road
Adelphi, MD 20783

Commander
Air Force Systems Command
ATTN: WER (Mr. Richard F. Picanso)
Andrews AFB, MD 20334

Martin Marietta Laboratories
ATTN: Jar Mo Chen
1450 South Rolling Road
Baltimore, MD 21227

Commander
US Army Concepts Analysis Agency
ATTN: CSCA-SMC (Mr. Hal E. Hock)
8120 Woodmont Avenue
Bethesda, MD 20014

Director
National Security Agency
ATTN: R52/Dr. Douglas Woods
Fort George G. Meade, MD 20755

Chief
Intelligence Materiel Development
& Support Office
US Army Electronic Warfare Laboratory
ATTN: DELEW-I (LTC Kenneth E. Thomas)
Fort George G. Meade, MD 20755

The Johns Hopkins University
Applied Physics Laboratory
ATTN: Dr. Michael J. Lun
John Hopkins Road
Laurell, MD 20810

Dr. Stephen T. Hanley
1720 Rhodesia Avenue
Oxon Hill, MD 20022

Science Applications Inc.
ATTN: Mr. G. D. Currie
15 Research Drive
Ann Arbor, MI 48103

Science Applications Inc.
ATTN: Dr. Robert E. Turner
15 Research Drive
Ann Arbor, MI 48103

Commander
US Army Tank-Automotive Research
& Development Command
ATTN: DRDTA-ZSC (Mr. Harry Young)
Warren, MI 48090

Commander
US Army Tank Automotive Research
& Development Command
ATTN: DRDTA-ZSC (Mr. Wallace Mick, Jr.)
Warren, MI 48090

Dr. A. D. Belmont
Research Division
Control Data Corporation
P.O. Box 1249
Minneapolis, MN 55440

Director
US Army Engr Waterways Experiment Station
ATTN: WESEN (Mr. James Mason)
P.O. Box 631
Vicksburg, MS 39180

Dr. Jerry Davis
Department of Marine, Earth
and Atmospheric Sciences
North Carolina State University
Raleigh, NC 27650

Commander
US Army Research Office
ATTN: DRXRO-GS (Dr. Leo Alpert)
P.O. Box 12211
Research Triangle Park, NC 27709

Commander
US Army Research Office
ATTN: DRXRO-PP (Brenda Mann)
P.O. Box 12211
Research Triangle Park, NC 27709

Commander
US Army Cold Regions Research
& Engineering Laboratory
ATTN: CRREL-RD (Dr. K. F. Sterrett)
Hanover, NH 03755

Commander/Director
US Army Cold Regions Research
& Engineering Laboratory
ATTN: CRREL-RG (Mr. George Aitken)
Hanover, NH 03755

Commander
US Army Cold Regions Research
& Engineering Laboratory
ATTN: CRREL-RG (Mr. Roger H. Berger)
Hanover, NH 03755

Commander
US Army Armament Research
& Development Command
ATTN: DRDAR-AC (Mr. James Greenfield)
Dover, NJ 07801

Commander
US Army Armament Research
& Development Command
ATTN: DRDAR-TSS (Bldg #59)
Dover, NJ 07801

Commander
US Army Armament Research
& Development Command
ATTN: DRCPM-CAWS-EI (Mr. Peteris Jansons)
Dover, NJ 07801

Commander
US Army Armament Research
& Development Command
ATTN: DRCPM-CAWS-EI (Mr. G. H. Waldron)
Dover, NJ 07801

Deputy Joint Project Manager
for Navy/USMC SAL GP
ATTN: DRCPM-CAWS-NV (CPT Joseph Miceli)
Dover, NJ 07801

Commander/Director
US Army Combat Surveillance & Target
Acquisition Laboratory
ATTN: DELCS-I (Mr. David Longinotti)
Fort Monmouth, NJ 07703

Commander/Director
US Army Combat Surveillance & Target
Acquisition Laboratory
ATTN: DELCS-PE (Mr. Ben A. Di Campli)
Fort Monmouth, NJ 07703

Commander/Director
US Army Combat Surveillance & Target
Acquisition Laboratory
ATTN: DELCS-R-S (Mr. Donald L. Foiani)
Fort Monmouth, NJ 07703

Director
US Army Electronics Technology &
Devices Laboratory
ATTN: DELET-DD (S. Danko)
Fort Monmouth, NJ 07703

Project Manager
FIREFINDER/REMBASS
ATTN: DRCPM-FFR-TM (Mr. John M. Bialo)
Fort Monmouth, NJ 07703

Commander
US Army Electronics Research
& Development Command
ATTN: DRDEL-SA (Dr. Walter S. McAfee)
Fort Monmouth, NJ 07703

OLA, 2WS (MAC)
Holloman AFB, NM 88330

Commander
Air Force Weapons Laboratory
ATTN: AFWL/WE (MAJ John R. Elrick)
Kirtland, AFB, NM 87117

Director
USA TRADOC Systems Analysis Activity
ATTN: ATAA-SL
White Sands Missile Range, NM 88002

Director
USA TRADOC Systems Analysis Activity
ATTN: ATAA-SL (Dolores Anguiano)
White Sands Missile Range, NM 88002

Director
USA TRADOC Systems Analysis Activity
ATTN: ATAA-TDB (Mr. Louie Dominguez)
White Sands Missile Range, NM 88002

Director
USA TRADOC Systems Analysis Activity
ATTN: ATAA-TDB (Mr. William J. Leach)
White Sands Missile Range, NM 88002

Director
USA TRADOC Systems Analysis Activity
ATTN: ATAA-TGP (Mr. Roger F. Willis)
White Sands Missile Range, NM 88002

Director
Office of Missile Electronic Warfare
ATTN: DELEW-M-STO (Dr. Steven Kovel)
White Sands Missile Range, NM 88002

Office of the Test Director
Joint Services EO GW CM Test Program
ATTN: DRXDE-TD (Mr. Weldon Findley)
White Sands Missile Range, NM 88002

Commander
US Army White Sands Missile Range
ATTN: STEWS-PT-AL (Laurel B. Saunders)
White Sands Missile Range, NM 88002

Commander
US Army R&D Coordinator
US Embassy - Bonn
Box 165
APO New York 09080

Grumman Aerospace Corporation
Research Department - MS A08-35
ATTN: John E. A. Selby
Bethpage, NY 11714

Rome Air Development Center
ATTN: Documents Library
TSLD (Bette Smith)
Griffiss AFB, NY 13441

Dr. Roberto Vaglio-Laurin
Faculty of Arts and Science
Dept. of Applied Science
26-36 Stuyvesant Street
New York, NY 10003

Air Force Wright Aeronautical Laboratories/
Avionics Laboratory
ATTN: AFWAL/AARI-3 (Mr. Harold Geltmacher)
Wright-Patterson AFB, OH 45433

Air Force Wright Aeronautical Laboratories/
Avionics Laboratory
ATTN: AFWAL/AARI-3 (CPT William C. Smith)
Wright-Patterson AFB, OH 45433

Commandant
US Army Field Artillery School
ATTN: ATSF-CF-R (CPT James M. Watson)
Fort Sill, OK 73503

Commandant
US Army Field Artillery School
ATTN: ATSF-CD-MS
Fort Sill, OK 73503

Commandant
US Army Field Artillery School
ATTN: ATSF-CF-R
Fort Sill, OK 73503

Commandant
US Army Field Artillery School
ATTN: NOAA Liaison Officer
(CDR Jeffrey G. Carlen)
Fort Sill, OK 73503

Commandant
US Army Field Artillery School
Morris Swett Library
ATTN: Reference Librarian
Fort Sill, OK 73503

Commander
Naval Air Development Center
ATTN: Code 301 (Mr. George F. Eck)
Warminster, PA 18974

The University of Texas at El Paso
Electrical Engineering Department
ATTN: Dr. Joseph H. Pierluissi
El Paso, TX 79968

Commandant
US Army Air Defense School
ATTN: ATSA-CD-SC-A (CPT Charles T. Thorn)
Fort Bliss, TX 79916

Commander
HQ, TRADOC Combined Arms Test Activity
ATTN: ATCAT-OP-Q (CPT Henry C. Cobb, Jr.)
Fort Hood, TX 76544

Commander
HQ, TRADOC Combined Arms Test Activity
ATTN: ATCAT-SCI (Dr. Darrell W. Collier)
Fort Hood, TX 76544

Commander
US Army Dugway Proving Ground
ATTN: STEDP-MT-DA-L
Dugway, UT 84022

Commander
US Army Dugway Proving Ground
ATTN: STEDP-MT-DA-M (Mr. Paul E. Carlson)
Dugway, UT 84022

Commander
US Army Dugway Proving Ground
ATTN: STEDP-MT-DA-T (Mr. John Trethewey)
Dugway, UT 84022

Commander
US Army Dugway Proving Ground
ATTN: STEDP-MT-DA-T (Mr. William Peterson)
Dugway, UT 84022

Defense Documentation Center
ATTN: DDC-TCA
Cameron Station Bldg 5
Alexandria, VA 22314
12

Ballistic Missile Defense Program Office
ATTN: DACS-BMT (Colonel Harry F. Ennis)
5001 Eisenhower Avenue
Alexandria, VA 22333

Defense Technical Information Center
ATTN: DDA-2 (Mr. James E. Shafer)
Cameron Station, Bldg 5
Alexandria, VA 22314

Commander
US Army Materiel Development
& Readiness Command
ATTN: DRCBSI-EE (Mr. Albert Giambalvo)
5001 Eisenhower Avenue
Alexandria, VA 22333

Commander
US Army Materiel Development
& Readiness Command
ATTN. DRCLDC (Mr. James Bender)
5001 Eisenhower Avenue
Alexandria, VA 22333

Defense Advanced Rsch Projects Agency
ATTN: Steve Zakanyez
1400 Wilson Blvd
Arlington, VA 22209

Defense Advanced Rsch Projects Agency
ATTN: Dr. James Tegnelia
1400 Wilson Blvd
Arlington, VA 22209

Institute for Defense Analyses
ATTN: Mr. Lucien M. Biberman
400 Army-Navy Drive
Arlington, VA 22202

Institute for Defense Analyses
ATTN: Dr. Ernest Bauer
400 Army-Navy Drive
Arlington, VA 22202

Institute for Defense Analyses
ATTN: Dr. Hans G. Wolfhard
400 Army-Navy Drive
Arlington, VA 22202

System Planning Corporation
ATTN: Mr. Daniel Friedman
1500 Wilson Boulevard
Arlington, VA 22209

System Planning Corporation
ATTN: COL Hank Shelton
1500 Wilson Boulevard
Arlington, VA 22209

US Army Intelligence & Security Command
ATTN: Edwin Speakman, Scientific Advisor
Arlington Hall Station
Arlington, VA 22212

Commander
US Army Operational Test
& Evaluation Agency
ATTN: CSTE-ED (Mr. Floyd I. Hill)
5600 Columbia Pike
Falls Church, VA 22041

Commander and Director
US Army Engineer Topographic Laboratories
ATTN: ETL-GS-A (Mr. Thomas Neidringhaus)
Fort Belvoir, VA 22060

Director
US Army Night Vision &
Electro-Optics Laboratory
ATTN: DELNV-L (Dr. Rudolf G. Buser)
Fort Belvoir, VA 22060

Director
US Army Night Vision &
Electro-Optics Laboratory
ATTN: DELNV-L (Dr. Robert S. Rodhe)
Fort Belvoir, VA 22060

Director
US Army Night Vision &
Electro-Optics Laboratory
ATTN: DELNV-VI (Mr. Joseph R. Moulton)
Fort Belvoir, VA 22060

Director
US Army Night Vision &
Electro-Optics Laboratory
ATTN: DELNV-VI (Luanne P. Obert)
Fort Belvoir, VA 22060

Director
US Army Night Vision
& Electro-Optics Laboratory
ATTN: DELNV-VI (Mr. Thomas W. Cassidy)
Fort Belvoir, VA 22060

Director
US Army Night Vision &
Electro-Optics Laboratory
ATTN: DELNV-VI (Mr. Richard J. Bergemann)
Fort Belvoir, VA 22060

Director
US Army Night Vision &
Electro-Optics Laboratory
ATTN: DELNV-VI (Dr. James A. Ratches)
Fort Belvoir, VA 22060

Commander
US Army Training & Doctrine Command
ATTN: ATCD-AN
Fort Monroe, VA 23651

Commander
US Army Training & Doctrine Command
ATTN: ATCD-AN-M
Fort Monroe, VA 23651

Commander
US Army Training & Doctrine Command
ATTN: ATCD-F-A (Mr. Chris O'Connor, Jr.)
Fort Monroe, VA 23651

Commander
US Army Training & Doctrine Command
ATTN: ATCD-IE-R (Mr. David M. Ingram)
Fort Monroe, VA 23651

Commander
US Army Training & Doctrine Command
ATTN: ATCD-M-I/ATCD-M-A
Fort Monroe, VA 23651

Commander
US Army Training & Doctrine Command
ATTN: ATDOC-TA (Dr. Marvin P. Pastel)
Fort Monroe, VA 23651

Department of the Air Force
OL-I, AWS
Fort Monroe, VA 23651

Department of the Air Force
HQS 5 Weather Wing (MAC)
ATTN: 5 WW/DN
Langley Air Force Base, VA 23655

Commander
US Army INSCOM/Quest Research Corporation
ATTN: Mr. Donald Wilmot
6845 Elm Street, Suite 407
McLean, VA 22101

General Research Corporation
ATTN: Dr. Ralph Zirkind
7655 Old Springhouse Road
McLean, VA 22102

Science Applications, Inc.
8400 Westpark Drive
ATTN: Dr. John E. Cockayne
McLean, VA 22102

US Army Nuclear & Chemical Agency
ATTN: MONA-WE (Dr. John A. Berberet)
7500 Backlick Road, Bldg 2073
Springfield, VA 22150

Director
US Army Signals Warfare Laboratory
ATTN: DELSW-EA (Mr. Douglas Harkleroad)
Vint Hill Farms Station
Warrenton, VA 22186

Director
US Army Signals Warfare Laboratory
ATTN: DELSW-OS (Dr. Royal H. Burkhardt)
Vint Hill Farms Station
Warrenton, VA 22186

Commander
US Army Cold Regions Test Center
ATTN: STECR-TD (Mr. Jerold Barger)
APO Seattle, WA 98733

HQDA (SAUS-OR/Hunter M. Woodall, Jr./
Dr. Herbert K. Fallin)
Rm 2E 614, Pentagon
Washington, DC 20301

COL Elbert W. Friday, Jr.
OUSDRE
Rm 3D 129, Pentagon
Washington, DC 20301

Defense Communications Agency
Technical Library Center
Code 222
Washington, DC 20305

Director
Defense Nuclear Agency
ATTN: Technical Library (Mrs. Betty Fox)
Washington, DC 20305

Director
Defense Nuclear Agency
ATTN: RAAE (Dr. Carl Fitz)
Washington, DC 20305

Director
Defense Nuclear Agency
ATTN: SPAS (Mr. Donald J. Kohler)
Washington, DC 20305

Defense Intelligence Agency
ATTN: DT/AC (LTC Robert Poplawski)
Washington, DC 20301

HQDA (DAMA-ARZ-D/Dr. Verderame)
Washington, DC 20310

HQDA (DAMI-ISP/Mr. Beck)
Washington, DC 20310

Department of the Army
Deputy Chief of Staff for
Operations and Plans
ATTN: DAMO-RQ
Washington, DC 20310

Department of the Army
Director of Telecommunications and
Command and Control
ATTN: DAMO-TCZ
Washington, DC 20310

Department of the Army
Assistant Chief of Staff for Intelligence
ATTN: DAMI-TS
Washington, DC 20310

HQDA (DAEN-RDM/Dr. de Percin)
Casimir Pulaski Building
20 Massachusetts Avenue
Room 6203
Washington, DC 20314

National Science Foundation
Division of Atmospheric Sciences
ATTN: Dr. Eugene W. Bierly
1800 G. Street, N.W.
Washington, DC 20550

Director
Naval Research Laboratory
ATTN: Code 4320 (Dr. Lothar H. Ruhnke)
Washington, DC 20375

Commanding Officer
Naval Research Laboratory
ATTN: Code 6009 (Dr. John MacCallum, Jr.)
Washington, DC 20375

Commanding Officer
Naval Research Laboratory
ATTN: Code 6530 (Mr. Raymond A. Patten)
Washington, DC 20375

Commanding Officer
Naval Research Laboratory
ATTN: Code 6533 (Dr. James A. Dowling)
Washington, DC 20375